Z. Phys. A 358, 73–80 (1997)

ZEITSCHRIFT
FÜR PHYSIK A

Shape of collective flow in highly central Au(150 A MeV)+Au collisions

C. Roy[11,⋆], C. Kuhn[11], J.P. Coffin[11], P. Crochet[11], P. Fintz[11], G. Guillaume[11], F. Jundt[11], C. Maazouzi[11], F. Rami[11], L. Tizniti[11], P. Wagner[11], J.P. Alard[3], V. Amouroux[3], Z. Basrak[13], N. Bastid[3], I. Belyaev[8], D. Best[4] J. Biegansky[10], A. Buta[1], R. Čaplar[13], N. Cindro[13], R. Donà[7], P. Dupieux[3], M. Dzelalija[13], Z.G. Fan[4], Z. Fodor[2], L. Fraysse[3], A. Gobbi[4], N. Herrmann[6], K.D. Hildenbrand[4], S. Hölbling[13], B. Hong[4], S.C. Jeong[4], J. Kecskemeti[2], M. Kirejczyk[4], P. Koncz[2], Y. Korchagin[8], R. Kotte[10], A. Lebedev[8,12], I. Legrand[1], Y. Leifels[4], V. Manko[9], G. Mgebrishvili[9], D. Moisa[1], J. Mösner[10], W. Neubert[10], D. Pelte[6], M. Petrovici[1], C. Pinkenburg[4], P. Pras[3], W. Reisdorf[4], J.L. Ritman[4], A.G. Sadchikov[9], D. Schüll[4], Z. Seres[2], B. Sikora[12], V. Simion[1], V. Smolyankin[8], U. Sodan[4], M. Trzaska[6], M. Vasiliev[9], G.S. Wang[4], J.P. Wessels[4], T. Wienold[4], D. Wohlfarth[10], A. Zhilin[8], J. Konopka[5], H. Stöcker[5]

[1] Institute for Physics and Nuclear Engineering, Bucharest, Romania
[2] Research Institute for Particles and Nuclear Physics, Budapest, Hungary
[3] Laboratoire de Physique Corpusculaire, IN2P3-CNRS, Université Blaise Pascal, Clermont-Ferrand, France
[4] Gesellschaft für Schwerionenforschung, Darmstadt, Germany
[5] Institut für Theoretische Physik der Universität Frankfurt, Frankfurt am Main, Germany
[6] Physikalisches Institut der Universität Heidelberg, Heidelberg, Germany
[7] Istituto Nazionale di Fisica Nucleare, Legnaro, Italy
[8] Institute for Theoretical and Experimental Physics, Moscow, Russia
[9] Russian Research Institute "Kurchatov", Moscow, Russia
[10] Forschungszentrum Rossendorf, Dresden, Germany
[11] Centre de Recherches Nucléaires, IN2P3-CNRS, Université Louis Pasteur, F-67037 Strasbourg, France
[12] Institute of Experimental Physics, Warsaw University, Warsaw, Poland
[13] Rudjer Boskovic Institute, Zagreb, Croatia

Received: 4 November 1996
Communicated by A. Schäfer

Abstract. Using the FOPI facility at GSI, charged particles ($1 \leq Z \leq 6$) produced in the Au(150 A MeV)+Au reaction have been measured at laboratory angles $1.2^0 < \Theta_{lab} < 30^0$. Highly central collisions have been selected with two criteria, both dealing with the longitudinal and transverse degrees of freedom of the reaction. The relevance of this selection method is supported by QMD calculations which indicate that such criteria are able to select mean impact parameters less than 2 fm. Bias effects introduced by the criteria have been evaluated. The centre-of-mass polar angle distributions of low energy clusters emitted in these central collisions, have been extracted : the intensity ratio deduced for a transverse to longitudinal emission is found to be $R=1.4^{+0.2}_{-0.4}$. Model comparisons using QMD are presented. The value of R appears to depend sensitively on the nucleon-nucleon cross section, σ_{nn}. Within this model, a value of $\sigma_{nn}=25\pm5$ mb is derived.

PACS: 25.70.-z

1 Introduction

The nuclear collective flow characterising the expansion phase in central heavy-ion collisions is nowadays one of the most studied phenomena [1-10] because it is expected to provide information on the properties of compressed and heated nuclear matter. In semi-central collisions at intermediate bombarding energies (a few hundreds of A MeV), these long time recognized collective effects [1] have been shown to be divided into two main components : the *side-splash* [2] dominantly contained in the reaction plane and the *squeeze-out* [3, 5] directed perpendicularly to it. When the impact parameter reduces to nearly zero, these two components are expected to merge.

Experiments based on the observation of clusters, performed with the FOPI-detector [11], have evidenced the presence of a mid-rapidity source in central collisions [12], with unexpected large cluster yields [13] and with collective energies an order of magnitude larger than for the directed flow [14, 15]. In this paper the question of the shape of the mid-rapidity source in highly central collisions is addressed with the hope to get some information on the nucleon-nucleon cross section σ_{nn}, a leading parameter when nuclear transparency comes into play.

Up to now, only few experimental analyses have been devoted to this topic and furthermore they have been generally restricted to light particles ($Z \leq 2$). Theoretical investigations are more numerous. Collective phenomena in head-on collisions have been predicted strongly accentuated transversally to the beam direction (oblate form in the phase space) since quite a long time by hydrodynamics [16] and more recently by microscopic dynamical calculations [17–19]. Other calculations [20, 21] advocate different scenarios, going from a forward-backward emission of the ejectiles, focussed along the beam axis (prolate form) up to a radial expansion (i.e. an isotropic emission).

The shape of the flow appears to be strongly connected to hard scattering, in other words to σ_{nn}. In the early hydrodynamical calculations, no viscosity was considered. At a microscopic level, this treatment would be synonymous with a high nucleon-nucleon cross section which leads to a large amount of stopping. As a consequence, these models predict

⋆ *Present address* : SUBATECH, Nantes, France

nuclear matter to be violently ejected transversally, leading to polar angle distributions in the centre-of-mass peaking around 90^0 and to transverse momenta larger than longitudinal momenta. This effect is confirmed by microscopic models like QMD [17] using a large nucleon-nucleon cross section.

The centre-of-mass polar angle Θ_{cm} is a suitable observable for studying the event shape in the span of low impact parameters. Indeed, its distribution is affected both by the longitudinal (reflecting the amount of stopping) and the transverse (created in the reaction) degrees of freedom. Hence, it indicates the main direction of nuclear matter flow, with no need for any reaction plane determination. For a small σ_{nn} value, the central event shape becomes forward-backward peaked with maxima at 0^0 and 180^0 in the dN/d(cosΘ_{cm}) distributions [20–22]. A peak at 90^0 expresses a large number of interactions (high σ_{nn}) between the nucleons of the projectile and the target while an intermediate σ_{nn} value implies that the emission becomes more or less isotropic in phase space (flat polar angle distributions). In view of the high sensitivity of the Θ_{cm} observable to the nucleon-nucleon cross section, the comparison between experimental and theoretical Θ_{cm} distributions should allow, at least, an estimate of σ_{nn}.

The present study has been performed by using the FOPI facility [11] at GSI (Darmstadt) operating in the so-called Phase I configuration. The data have been collected for charged particles $1 \leq Z \leq 6$ emitted in the Au(150 A MeV)+Au reaction at laboratory angles $1.2^0 < \Theta < 30^0$, which cover the major part of the forward hemisphere in the centre-of-mass frame.

At variance with previous experiments dominantly based on light product measurements ($Z \leq 3$) [1, 23, 24], the present investigation deals with cluster measurements. The cluster yields of the centre-of-mass polar angle distributions are investigated in detail for central collisions, while the polar angle dependence of the kinetic energies of clusters is presented in a separate report together with bombarding energy dependence of the general features of the mid-rapidity source [25]. In order to lessen present limitations of FOPI-Phase I, the yields are selected for centre-of-mass kinetic energies, E_{kin} less than 9 A MeV.

Since the investigated effects are expected to manifest themselves only for very small impact parameters ($b \leq 2$ fm), various centrality criteria are examined and the most effective is retained, even at cost of possible biases. The biases are then evaluated using calculations based on a specific QMD theoretical approach [17].

2 Selection of highly central collisions

Since the impact parameter b cannot be measured experimentally, the degree of centrality of the reaction has to be evaluated by means of criteria defined from experimental observables whose distributions vary significantly with b. Very low impact parameter collisions occur seldom while the analysis requires significant statistics. One has also to pay attention to the fact that by nature, any centrality criterion will influence the shape or other characteristics of the selected events in several manners. Different criteria will lead to the selection of different subsets of events. Due to distortions introduced by the criteria, the experimentally selected set of central collisions will depart somewhat from that of the "true" central events (i.e. those selected according to the value of their impact parameter). The evaluation of these distortion effects may be achieved by comparing both ensembles of events (corresponding to the same reaction cross section) in the framework of the QMD model. Following earlier works, the FOPI collaboration has developed several criteria aimed at the selection of central collisions. Their merits and drawbacks have been discussed elsewhere [26]. In the present work, we aim at the highest possible centrality selection. We will first reexamine the already existing criteria in this context before introducing a new one.

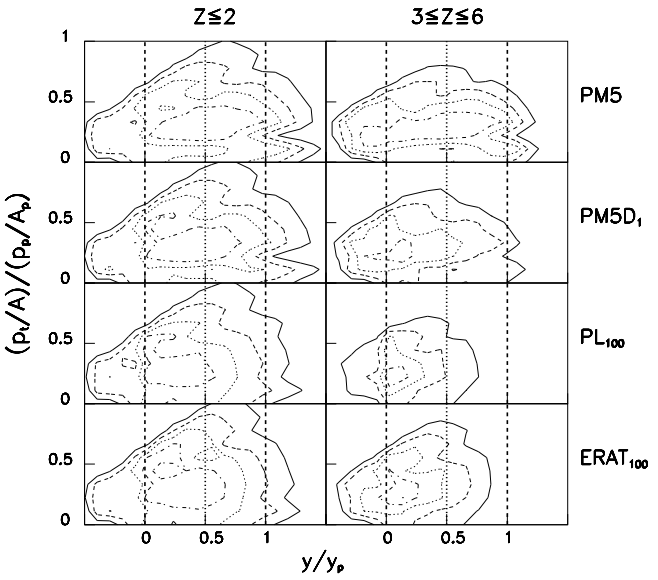

Fig. 1. Transverse momentum per nucleon (p_t/A) of the ejectiles (expressed in units of the projectile momentum per nucleon (p_p/A_p) in the centre-of-mass system) as a function of the ejectile rapidity (y) (normalised to that of the projectile (y_p) in the centre-of-mass frame) for different criteria of centrality for the Au(150 A MeV)+Au reaction. Lighter $Z \leq 2$ (*left column*) and heavier $3 \leq Z \leq 6$ (*right*) ejectiles are considered. Contour plots for PM5, $PM5D_1$, PL_{100} and $ERAT_{100}$ are shown from *top* to *bottom*. The contours correspond to 20, 40, 60, 80 % of the maximum of the invariant cross section from outer to inner

Among the most frequently used event selections, one may start from the one based on charged particle multiplicities. The most violent reactions imply a large desintegration of the colliding system, thus high charged particle multiplicities (PMUL). This approach was followed earlier in the Plastic Ball experiments [1-4]. It was recently used in the FOPI experiments by considering the PM5 criterion [12], defined at 150 A MeV with the condition PMUL>36 (for $7^0 < \Theta_{lab} < 30^0$), leading to a cross section of 280 mb. According to QMD calculations [21], the impact parameter for PM5 events ranges from 0 up to 7 fm ($<b> \sim 3.5$ fm) [12]. A higher multiplicity requirement does not lead to a significant reduction of the impact parameter, while lowering substantially the cross section (100 mb) [27]. The PM5 criterion depends only on the degree of dissociation of the system. No consideration about the event shape is implied. It turns out that many events still contain ejectiles with rapidity close to that of the projectile. This characteristic can be seen in Fig.1, showing results obtained for the Au(150 A MeV) +Au reaction. Here, the transverse linear momentum per nucleon, expressed in units of projectile

linear momentum per nucleon in the centre-of-mass system, plotted as a function of the rapidity scaled to that of the projectile, is shown for light particles Z≤2 (left column) and for clusters Z≥3 (right column). One may observe that spectator remnants are clearly present like in typical semi-central collisions. Hence, a criterion based only on the charged particle multiplicities suffers an obvious limitation for a selection of central events.

In order to reach lower impact parameters, an additional criterion was used. When b tends to zero, the disappearance of the reaction plane leads to transverse momenta of the ejectiles emitted in the forward hemisphere, homogeneously distributed in the azimuthal plane. This led previous authors to define the directivity [12, 28], event by event, as :

$$D = \left| \sum_i \mathbf{p_t^i} \right| \Big/ \sum_i |\mathbf{p_t^i}| \Bigg]_{y \geq 0}$$

where the sum runs over the transverse momentum $\mathbf{p_t^i}$ of all detected particles emitted in the forward hemisphere of the centre-of-mass (y≥0) within an event. High centrality should yield low directivity; thus, the condition D_1 (D≤0.2) may be added to the PM5 preselection [12]. QMD calculations [21] have been performed to evaluate the mean impact parameter reached with the $PM5D_1$ criterion. They yield a value of 2.8 fm. However, the dependence of the directivity on the impact parameter [12, 27] is such that events corresponding to b∼ 5-7 fm remain present to some extent, with the extra D_1 condition. It results from the fact that semi-central events may include projectile remnants ejected with a large longitudinal momentum and a weak transverse one, hence contributing only little to the directivity value. The effectiveness of $PM5D_1$ may be seen in Fig.1 (2^{nd} row). When compared with PM5, the $PM5D_1$ distributions are shifted towards mid-rapidity, especially for Z≥3, so enlightening the marked sensitivity of clusters to the impact parameter. Nevertheless, a non negligible component near the projectile rapidity still remains.

In order to better isolate the mid-rapidity source corresponding to the most central events, we have looked for more constraining criteria.

By definition, the collisions at b=0 imply the non-existence of projectile and target remnants since the whole colliding system participates in the reaction. This fact can be used by requiring a low global longitudinal momentum or a large global transverse to longitudinal energy ratio when considering all the particles emitted in the forward hemisphere within an event. Setting conditions on longitudinal and transverse momenta may influence more directly the shape of the mid-rapidity source and introduce more distortions than cuts on multiplicity and directivity, these latter quantities being less directly related with the event shape. First, we shall investigate the selectivity power and later we will evaluate the distortions.

Let us define, event by event, the quantity PL :

$$\mathrm{PL} = \left[\frac{\sum_i p_l^i}{Z_{tot}} \right]_{y \geq 0}^{p_t \leq 0.6}$$

where $\sum_i p_l^i$ is the sum running over all particle centre-of-mass longitudinal momenta and Z_{tot} is the corresponding total charge measured in the forward hemisphere of the centre-of-mass (y≥0). To avoid background contamination, we will consider only events for which the detected charged particle multiplicity is larger than PMUL=18 (i.e. the so-called PM3, PM4 and PM5 bins [12]). In order to minimize the influence of the detector boundary limit at $\Theta_{lab} = 30^0$, the sum runs only over products whose $p_t \leq 0.6$ (where $p_t = p_t/A/p_p/A_p$ with A_p and p_p being the mass and the linear momentum in the centre-of-mass system of the projectile, respectively) independently of rapidity. The distribution of PL shown in Fig.2 is broad, extending from 0.1 up to 0.6 GeV/c per charge unit with a mean value of 0.33 GeV/c. By restraining PL to less than 0.257 GeV/c, one selects an ensemble of collisions corresponding to a cross section σ_{PL} of 100 mb (the criterion called PL_{100}). This cut represents a compromise between a high degree of centrality and acceptable statistics.

The result of using this criterion is illustrated in Fig.1 (3^{rd} row). One may still observe some contribution up to $y=y/y_p \sim 1$ for light particles, while for clusters the distribution is narrow and essentially located in the so-called participant region (y≤0.5), revealing a substantial reduction of the spectator component. These trends indicate clearly that the PL_{100} criterion selects, as expected, more effectively the mid-rapidity region than PM5 and $PM5D_1$.

In order to evaluate the degree of centrality obtained with the PL_{100} criterion, we have performed filtered QMD calculations [17]. The correlation between the average impact parameter <b> and the cross section σ_{PL}, relative to the PL

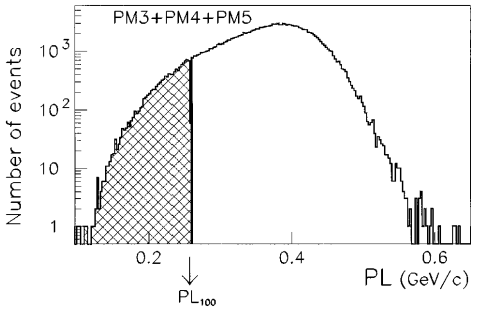

Fig. 2. Distribution of the PM3+PM4+PM5 events as a function of PL. The PL_{100} cut corresponds to the PL<0.257 condition, yielding a reaction cross section of 100 mb

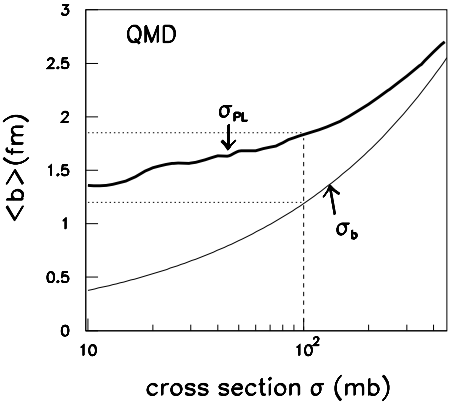

Fig. 3. Distribution of the average impact parameter <b> as a function of the cross section σ_{PL} corresponding to the PL event selection (*thick solid curve*), as predicted by QMD for Au+Au at 150 A MeV. The dependence of <b> on the geometrical cross section σ_b is also shown (*light solid curve*)

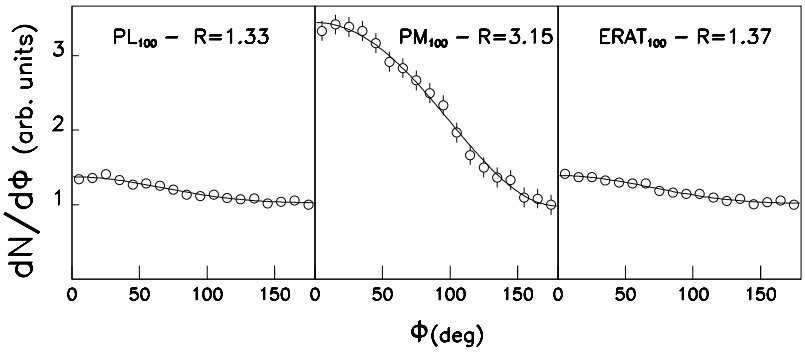

Fig. 4. Azimuthal angle distributions of ejectiles for Au(150 A MeV)+Au reactions selected with the PL_{100} (*left frame*), PM_{100} (*middle*) and $ERAT_{100}$ (*right*) conditions. The ϕ angle is defined with respect to a reference angle, calculated event by event and corresponding to the main direction of particule emission in the azimuthal plane. The *solid curves* are fits to the data with a polynomial function g (see text). Asymmetry ratios $R=g(0^0)/g(180^0)$ are also indicated

selection, is given in Fig.3. For purpose of comparison, <b> is also shown as a function of the geometrical cross section σ_b. This simulation demonstrates that a selected cross section σ_{PL} of 100 mb leads to a mean impact parameter of 1.8 fm (for σ_b=100 mb, <b>=1.2 fm in case of the true geometrical cross section). Thus, the PL_{100} criterion allows a low impact parameter selection with acceptable statistics.

As stated before, in the most central collisions where no preferential azimuthal emission should exist, the distribution of the azimuthal angle ϕ should be close to isotropy. This is indeed observed when the PL_{100} condition is applied to the data, as shown in Fig.4 (left frame). A polynomial fit to the data (curve) allows the estimation of the anisotropy of the distribution by calculating the ratio $R=g(0^0)/g(180^0)$ where g is the fit function ($g(\phi)=a_0+a_1\cos\phi+a_2\cos 2\phi$). As reported in the figure, R is equal to 1.33 for PL_{100}, while for the ejectiles emitted in PM_{100} reactions (charged particle multiplicity selection corresponding to a cross section of 100 mb) this ratio is as large as 3.15 (middle frame).

The PL criterion is to be compared with another cut operating on energy instead of linear momentum and which was used in previous analyses [26, 29]. It is the so-called ERAT criterion defined event by event, as :

$$ERAT = \sum_i E_t^i \Big/ \sum_i E_l^i \Big]_{y\geq 0}$$

where E_t^i and E_l^i are respectively, the transverse and longitudinal centre-of-mass kinetic energy of the particles emitted in the forward hemisphere in the centre-of-mass. High ERAT values mean that a large fraction of the initial longitudinal beam energy has been transfered into the transverse degree of freedom.

A cross section of 100 mb may be selected by imposing ERAT to be larger than 0.78. The result of using this condition ($ERAT_{100}$) is somewhat comparable with that obtained with PL_{100} as it can be observed in Fig.1 (bottom row). Following QMD calculations [21], the mean impact parameter achieved with the $ERAT_{100}$ is found equal to 2.1 fm.

The $dN/d\phi$ distribution of $ERAT_{100}$ collisions is shown in Fig.4 (right frame). They exhibit a weak asymmetry (R=1.37) quite comparable to that measured for PL_{100} events. Hence, it appears that the PL_{100} and $ERAT_{100}$ centrality criteria are more suitable for selecting low impact parameters than the PM_{100} and $PM5D_1$ criteria.

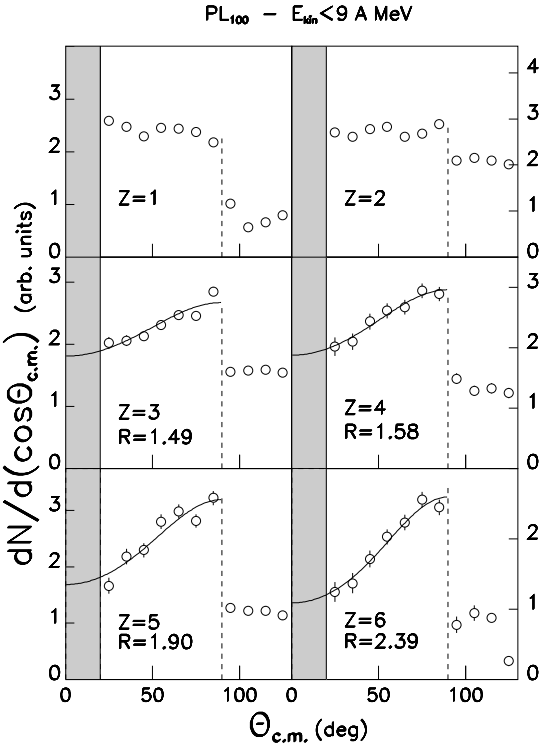

Fig. 5. Centre-of-mass polar angle distributions for ejectiles $1\leq Z\leq 6$ selected with the conditions PL_{100} and E_{kin} <9 A MeV. The grey zones correspond to the region where accurate corrections of acceptance and threshold effects are difficult, hence no data are considered. The *curves* are fits to the data. The brutal change around 90^0 is due to an autocorrelation effect (see text). Asymmetry ratios are calculated from 0^0 and 90^0 yields

3 Experimental centre-of-mass polar angle distributions

We have extracted the $dN/d(\cos\Theta_{cm})$ distributions of events selected with the PL_{100} criterion. They are shown in Fig.5, for ions $1\leq Z\leq 6$, after correction for low local inefficiencies of the detector. In order to avoid distortions due to the Θ_{lab} = 30^0 boundary limit of the detector, the distributions are limited to particles whose centre-of-mass kinetic energy (E_{kin}) is less than 9 A MeV. Besides, the distributions cannot be corrected with full accuracy and confidence below Θ_{cm} = 20^0 (grey zones in Fig.5). Indeed, a large fraction of the $0^0 \leq \Theta_{cm} \leq 10^0$ region resides below the ($\Theta_{lab} < 1.2^0$) lower acceptance limit of the detector while the $10^0 \leq \Theta_{cm} \leq 20^0$ domain is affected by efficiency loss, difficult to evaluate accurately. Hence no data is considered in this angular span.

As seen from Fig.5, for hydrogen and helium ions, the distributions are almost isotropic, whereas for clusters they are characterized by an asymmetry and a monotonic increase between 20^0 and 90^0. The higher the Z, the larger the effect. In order to quantify this effect, the cluster distributions between 20^0 and 90^0 have been fitted with a function (solid curves in Fig.5) defined as :

$$f(c, d, \Theta_{cm}) = c.e^{-d(\cos\Theta_{cm})^2}$$

The magnitude of the anisotropy effect between 0^0 and 90^0 is given by the factor $R = f(90^0)/f(0^0) = e^d$, also reported in the figure.

Speaking about possible distortions in the final result, as a consequence of a specific choice in a preselection of events, two types of effects may be mentioned : (i) the autocorrelation effect due to the inclusion of the particle of interest for the final result in the preselection, as it has been extensively discussed for the case of the reaction plane determination [30] and (ii) biases which influence in a more general way the final result. Both effects carry also a "finger print" of the limits in phase space which were used for the preselection (e.g the limits in the p_t-y plane). In principle, the autocorrelation effect can be eliminated by dropping the particle of interest (POI) from the preselection. However in this analysis, the POI has not been eliminated : this in order to preserve the highest possible centrality selectivity. The overall distortions have been evaluated on the basis of QMD calculations.

The sudden step in the angular distributions around 90^0 for PL_{100} events is due to an autocorrelation. Indeed the PL criterion favours the selection of reactions where particles are ejected preferentially in the forward hemisphere, hence a lack of counts beyond 90^0 in the dN/d(cosΘ_{cm}) distributions. The following qualitative rational allows to figure out the reason for this effect. Let us consider an event (a) whose particles are emitted mainly in the forward hemisphere of the centre-of-mass frame and let us suppose that this event belongs to the PL_{100} set. Let us consider now the same event, mirrored with respect to the mid-rapidity axis (event (b)), i.e the particles are now dominantly emitted in the backward hemisphere. Since only ejectiles emitted in the forward hemisphere contribute to the PL determination, the PL value relative to (b) will be generally larger than for (a). Hence, in many cases, when event (a) fullfills the PL$<$0.257 condition, the mirrored event (b) does not.

The analysis for fragments $3\leq Z\leq 6$ is summarized in Fig.6, together with similar studies conducted by using $ERAT_{100}$, $PM5D_1$ and PM5 cuts. The following points may be stressed : i) For $ERAT_{100}$, the discontinuity around 90^0 also exists but appears reduced as compared with that found in PL_{100}. It appears as a shift of the peak in the Θ_{cm} distribution toward values around 70^0. This shift is related to the phase space limitation of longitudinal and transverse momenta entering in the ERAT-selection : the maximum p_t varies with the rapidity according to the Θ_{lab} = 30^0 acceptance limit of the detector. Consequently, requiring large ERAT values privileges events for which the particle emission is focussed near $\Theta_{cm} \sim 70^0$. ii) In order to quantify the magnitude of the anisotropy, the fragment distributions have been fitted (solid curves) with the function f(c,d,Θ_{cm}) and the asymmetry ratios R=f(90^0)/f(0^0) and R=f(70^0)/f(0^0) have been extracted as R=1.73 and 1.60 for the PL_{100} and $ERAT_{100}$, respectively. Both distributions

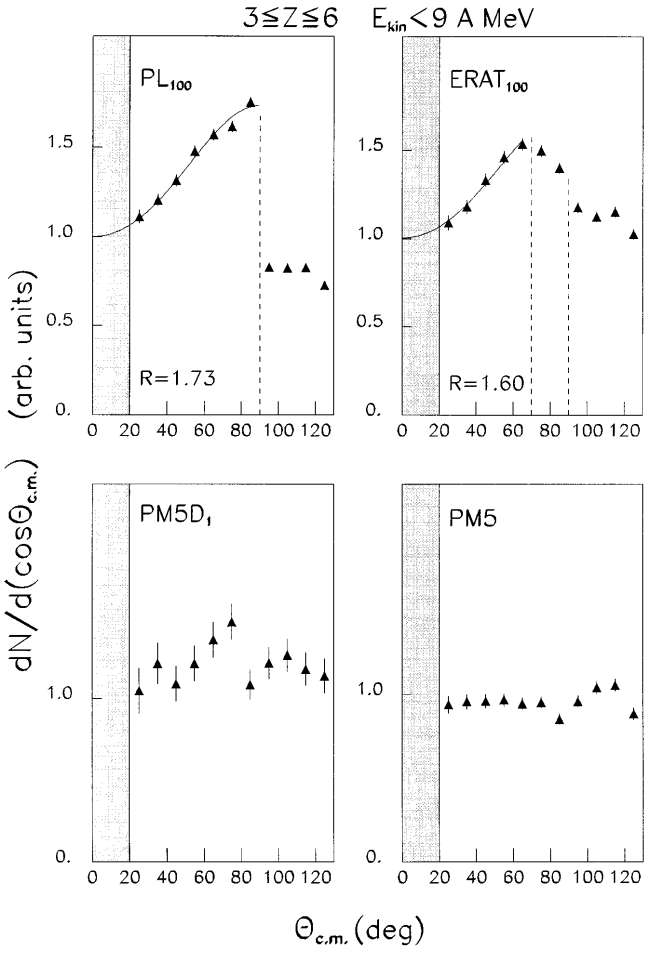

Fig. 6. Centre-of-mass polar angle distributions for fragments $3\leq Z\leq 6$ obtained with different centrality criteria : PL_{100}, $ERAT_{100}$, $PM5D_1$ and PM5. For the first two cuts, fits to the data are performed. The asymmetry ratios are calculated between 0^0 and 90^0 for the distribution relative to PL, and between 0^0 and 70^0 for the ERAT one

show a comparable asymmetry. iii) The asymmetry of the distributions becomes much smaller for $PM5D_1$ and vanishes for PM5. These trends indicate that when going to less central collisions, the transverse expansion weakens. The distributions do not exhibit any drop-off around Θ_{cm} = 90^0 : these criteria do not deal with either longitudinal or transverse degree of freedom.

4 Bias estimation

Before interpreting the polar angle distribution of clusters, one has to examine the possibility of distortions introduced by the used cuts.

The PL_{100} ($ERAT_{100}$) criterion selects events for impact parameters below 1.8 fm but includes also as many events for which b$>$ 1.8 fm, because of the fluctuations around this averaged value. As a result, it is essential to quantify the difference between the behaviour characterizing the experimentally selected events and that of "true" central events (i.e. selected according to the geometrical cross section). This can be achieved only in the framework of model simulations. Here, it was per-

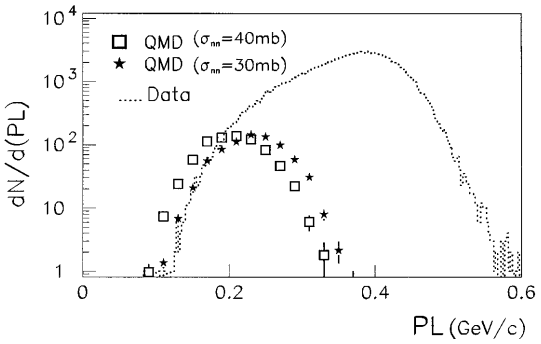

Fig. 7. Distributions of the PL quantity, predicted by the QMD model, for the Au+Au reactions at 150 A MeV whose the impact parameter ranges from 0 up to 4 fm. Two parametrisations of the nucleon-nucleon cross section are used : σ_{nn}=30 mb (*stars*) and 40 mb (*squares*). The former compares well with the experimental distribution (*dotted histogram*) in the low PL region

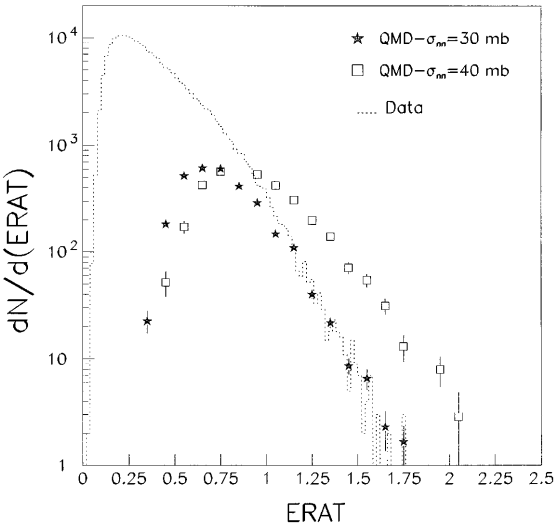

Fig. 8. Similar analysis as shown in Fig.7 for the ERAT instead of PL

formed by making use of QMD calculations [17]. Of course, one has to take into account the fact that the bias corrections will depend on the model inputs. In principle, a better bias estimation should be obtained with the set of parameters of the model which reproduces best the experimental data.

The experimental PL (Fig.7) and ERAT (Fig.8) distributions (dotted histograms) are compared to the corresponding QMD calculations in which the impact parameter is ranging from 0 to 4 fm and for two different parametrisations of σ_{nn}. It appears that a good agreement between data and calculations is obtained for σ_{nn}=30 mb over the PL and ERAT domains concerned by the span of b's. Conversely, a value of 40 mb for σ_{nn} leads to a poorer agreement. Hence, for the bias estimation, we will use QMD calculations utilizing σ_{nn}=30 mb.

The QMD dN/d(cosΘ_{cm}) distributions (solid dots) of the fragments 3≤Z≤6 calculated by selecting with the PL (left frame) and ERAT (right) criteria, a set of events corresponding to a cross section of 100 mb, are shown in Fig.9. They are compared with those obtained (squares) when considering "true" central events, with an equivalent geometrical cross section of 100 mb. The condition on the kinetic energy (E_{kin} < 9 A MeV) is, of course, systematically applied. Let us notice that the theoretical dN/d(cosΘ_{cm}) distribution related to the

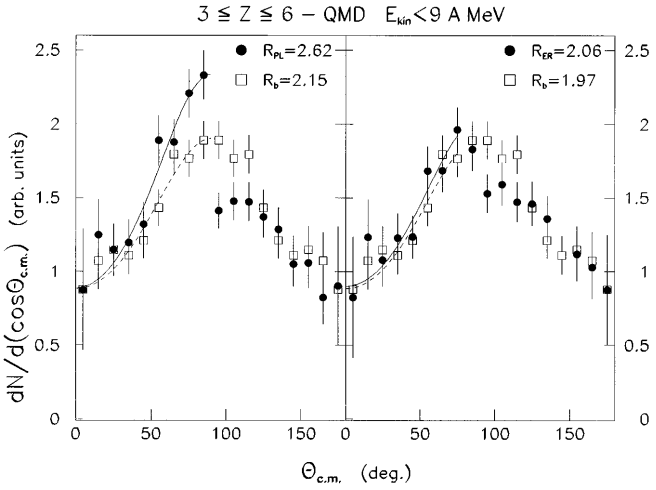

Fig. 9. Centre-of-mass polar angle distributions calculated with QMD for the 3≤Z≤6 fragments. The *squares* are for "true" central collisions corresponding to a mean impact parameter <b>=1.2 fm. In order to benefit the largest possible statistics, all the generated events have been summed in the forward hemisphere and mirrored into the backward. The *dots* are for events selected with PL (*left frame*) and ERAT (*right*) criteria. All distributions correspond to a reaction cross section of 100 mb. The *curves* are fits to the calculated distributions. The reported asymmetry factors, deduced from the fits, are obtained from the yield ratios (f(90^0)/f(0^0)) and (f(70^0)/f(0^0)) for the PL and ERAT sets of events, respectively

theoretical PL events, reproduces rather well the discontinuity at Θ_{cm} = 90^0 observed in the experimental data, while, as expected, it is not observed in the "true" central event distribution.

The departure between the distribution relative to the PL events and that of the "true" central's has been quantified by comparing the ratios R_{PL} (PL events) and R_b ("true" central's) obtained as described before. The distortion relative to the PL cut is given by the factor R_{bias}=R_b/R_{PL}=2.15/2.62=0.82 which, applied to the asymmetry factor extracted from the data (R=1.73), leads to a corrected value of $1.4^{+0.2}_{-0.4}$. To the extent that the model predicts an anisotropy larger than the one actually measured (see Fig.5 and Fig.9), we have set an asymmetric error on the σ_{nn} value.

It is worth seeing how this distortion effect varies with the value of the selected σ_{PL} cross section. When applying a more severe cut to PL to reduce the reaction cross section to 50 mb, the data show a larger raw anisotropy (R=2.11) but the distortion also increases so that the net asymmetry effect remains close to 1.4. This may be explained by the fact that dealing with less than 100 mb does not lower significantly the mean impact parameter (see Fig.3). Besides, due to fluctuations, the set of events is less and less typical of the true set of central collisions.

5 Model comparison and nucleon-nucleon cross section evaluation

The trend of the dN/d(cosΘ_{cm}) distribution in head-on collisions depends strongly on the degree of stopping of the nuclear matter. According to QMD, it is mainly governed by the

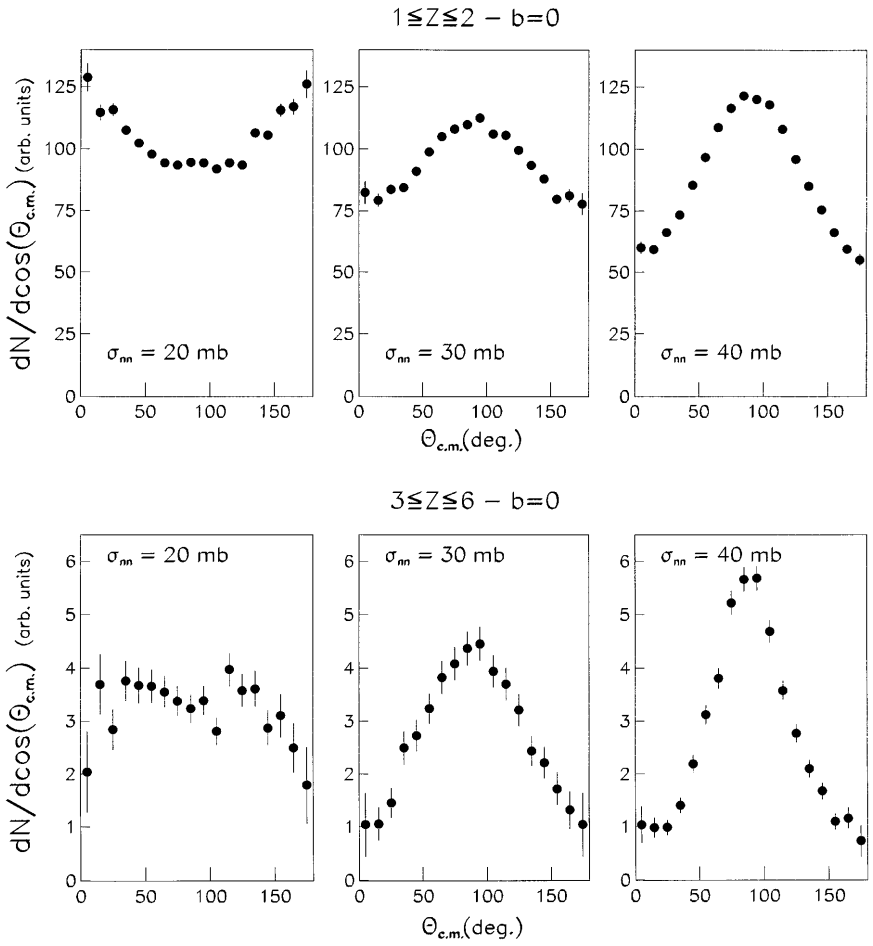

Fig. 10. Centre-of-mass polar angle distributions predicted by QMD for light particles (*upper frame*) and for fragments (*lower*) for the Au(150 A MeV)+Au reaction at b=0. Calculations are done for three parametrisations of the nucleon-nucleon cross section : σ_{nn}=20, 30 and 40 mb

nucleon-nucleon cross section σ_{nn} and only weakly by the parametrisation of the Equation of State [1, 17].

Some typical trends calculated for Z$\leq$2 and 3$\leq$Z$\leq$6 are shown in Fig.10 for σ_{nn} = 20, 30 and 40 mb. A drastic evolution is observed. Low σ_{nn}, i.e. some transparency, creates a prolate deformation of the event shape in the p_t-y plane resulting in a dN/dcos(Θ_{cm}) distribution peaking at Θ_{cm} = 0^0 and 180^0 for Z$\leq$2 and remaining roughly flat for heavier Z's. As σ_{nn} increases, both distributions peak around Θ_{cm} = 90^0 and the larger the cross section the more pronounced the effect. We have already shown that σ_{nn}=30 mb allows a satisfactory reproduction of the experimental PL and ERAT distributions in the region of low b's (see Figs.7 and 8) and that larger σ_{nn} value deteriorates the agreement. Comparison of Fig.5 and Fig.10, corresponding to measured and calculated centre-of-mass polar angle distributions, may allow to set some limits on σ_{nn}. This comparison for Z$\leq$2 and 3$\leq$Z$\leq$6 suggests in both cases a σ_{nn} of about 25$\pm$5 mb. Such an estimate is model dependent. However, recent QMD developments [17, 31] show that a careful treatment of the input parameters, in order to prepare the initial system of the collision in comparable conditions, leads to equivalent predictions regardless the QMD approach used.

6 Conclusion

In this work, we have analysed the collective flow in highly central Au(150 A MeV)+Au reactions, with emphasis on cluster (Z$\geq$3) flow.

The selection of very central collisions has been achieved by making phase space cuts utilizing the concept that highly central collisions must exhibit event shapes with vanishing spectator component. Two criteria have been examined, ERAT (requiring high transverse kinetic energy) and PL (low global longitudinal momentum). By restraining the reaction cross section to 100 mb, central collisions have been selected. We have shown that in these conditions, according to QMD calculations, the mean impact parameter reaches values less than 2 fm. Furthermore, phase space distributions in the transverse momentum-rapidity plane are centered at mid-rapidity and the azimuthal distributions present a weak asymmetry, thus confirming the high degree of centrality of the selected events.

The experimental centre-of-mass polar angle distributions of such events show an increase between 0^0 and 90^0 when the low energy clusters are considered. Distortion effects inherent to the centrality criteria have been studied using QMD calculations. These latter have been performed with an isotropic

nucleon-nucleon cross section allowing the model to reproduce well both experimental PL and ERAT distributions. The dN/d(cosΘ_{cm}) distributions, corrected for distortions, show an anisotropy value of $1.4^{+0.2}_{-0.4}$. A value of about 25 ± 5 mb for the in medium nucleon-nucleon scattering cross section, σ_{nn}, which is of basic importance for the stopping mechanism, has been derived from the data. This study should be considered as a first attempt to characterise the flow pattern in highly central collisions and subsequently to evaluate σ_{nn}. The present results which suffer some acceptance and efficiency lacks should be substantiated by further analyses with FOPI-Phase II.

References

1. A NATO Advanced Study Institute on the Nuclear Equation of State, Peniscola, Spain, ed. W. Greiner and H. Stöcker, NATO ASI Series B : Physics 216A and B (1989)
   See also : High Energy Nuclear Collisions, The GSI-LBL-Collaboration at the BEVALAC papers 1975-87, ed. H. H. Gutbrod, A. Sandoval, R. Stock, GSI-87-10 Report.
2. H. A. Gustafsson et al., Phys. Rev. Lett. **52**, 1590 (1984)
3. H. H. Gutbrod et al., Phys. Lett. **B216**, 267 (1989)
4. H. H. Gutbrod et al., Rep. Prog. Phys. **52**, 1267 (1989)
5. M. Desmoulins et al., Phys. Lett. **B241**, 476 (1990)
6. G. D. Westfall et al., Phys. Rev. Lett. **71**, 1986 (1993)
7. M. J. Huang et al., MSUCL-1024
8. J. P. Sullivan et al., Phys. Lett. **B249**, 8 (1990)
9. W. Q. Shen et al., Nucl. Phys. **A551**, 333 (1993)
10. A. Buta et al., Nucl. Phys. **A584**, 397 (1995)
11. A. Gobbi and the FOPI Collaboration, Nucl. Inst. Meth. **A324**, 156 (1993)
12. J. P. Alard and the FOPI Collaboration, Phys. Rev. Lett. **69**, 889 (1992)
13. C. Kuhn and the FOPI Collaboration, Phys. Rev. **C48**, 1232 (1993)
14. S. C. Jeong and the FOPI Collaboration, Phys. Rev. Lett. **72**, 3468 (1994)
15. M. Petrovici and the FOPI Collaboration, Phys. Rev. Lett **74**, 5001 (1995)
16. W. Scheid et al., Phys. Rev. Lett. **21**, 1479 (1968). For a review, see : H. Stöcker and W. Greiner, Phys. Rep. **137**, 277 (1986)
17. J. Konopka et al., Proc. of the Fifth International Conference on Nucleus Nucleus Collisions, Taormina (1994)
    J. Konopka, PhD Thesis, Frankfurt (1996)
    J. Konopka et al., to be published
18. P. Danielewicz, Phys. Rev. **C51**, 716 (1995)
19. B. Heide et al., Nucl. Phys. **A588**, 918 (1995)
20. W. Bauer, Phys. Rev. **C47**, R1838 (1993)
21. C. Hartnack et al., Nucl. Phys. **A495**, 303 (1989)
22. A. S. Botvina et al., Yad. Fiz. **58**, 1703 (1995)
23. M.A. Lisa and the EOS Collaboration, Phys. Rev. Lett. **75**, 2662 (1995)
24. G. Claesson et al., Phys. Lett. **B251**, 23 (1990)
25. W. Reisdorf and the FOPI Collaboration, to be published
26. W. Reisdorf for the FOPI Collaboration, Proc. of the XXII Int. Workshop on Gross Properties of Nuclei and Nuclear Excitation, Hirschegg, Austria (1994)
27. C. Roy, PhD Thesis, CRN96-08, Strasbourg, France (1996)
28. P. Beckmann et al., Mod. Phys. Lett. **A2**, 163 (1987)
29. N. Herrmann and the FOPI Collaboration, Nucl. Phys. **A553**, 739c (1993)
30. P. Danielewicz and G. Odyniec, Phys. Lett. **B157**, 146 (1985)
31. S.A. Bass, Proc. of the International Conference on Nuclear Physics at the Turn of the Millennium : Structure of Vacuum and Elementary Matter, Wilderness, South Africa (1996)